Indian Journal of Pure & Applied Physics
Vol. 64, May 2026, pp. 519-523
DOI: 10.56042/ijpap.v65i5.27306

DC Magnetron Sputtered Oxygenated Graphitic Carbon Nitride Synthesis Without Oxygen Doping

Soumik Kumar Kundu*, Samit Karmakar & Gouranga Sundar Taki
Institute of Engineering and Management, University of Engineering and Management Kolkata 700 091, India

Received: 6th January 2026; accepted: 12th March 2026

This study presented a novel synthesis of oxygenated graphitic carbon nitride thin films via DC magnetron sputtering, achieved without any intended oxygen supply from outside. Oxygen incorporation was occurred through residual gases i.e., atomic oxygen, hydroxyl radicals, water vapor, and CO_2, trapped in the deposition chamber. The synthesis environment was carefully analyzed using a Quadrupole Residual Gas Analyzer (QRGA). This approach minimized defect formation typically associated with external oxygen supply. The resulting films were characterized using X-ray photoelectron spectroscopy (XPS), Raman spectroscopy, and UV-Vis spectroscopy to confirm successful oxygen integration.

Keywords: Oxygenated graphitic carbon nitride, DC magnetron sputtering, Residual gas analysis

1 Introduction

Graphitic carbon nitride (g-C_3N_4) has become a popular photocatalyst because it is cheap, stable in chemicals, and has a good visible-light bandgap (~2.7 eV)[1]. But relatively low visible-light utilization efficiency[2] was observed in pure g-C_3N_4. Doping with elements, especially oxygen, was widely used because of its highly electronegativity has the capability of lowering the bandgap to improve its optical and photocatalytic efficiency[3,4]. The term, oxygenated graphitic carbon nitride used here, specifically implied the oxygen induced g-C_3N_4 and the term oxygen doping implied oxygen addition by external oxygen supply. There were some research works reported the common ways to develop oxygenated g-C_3N_4 by adding oxygen intentionally, like acid oxidation[5], heat treatment with oxalic acid[6], hydrothermal synthesis[7], co-precipitation[8], ion exchange[9], chemical vapour deposition[10,11] and cold plasma[12] etc. In these aforementioned techniques, there were some limitations like often usage of harsh chemicals, poor homogeneity and high costings. It was also observed from the study, the adding oxygen intentionally from the outside induced defect in the structure.

The motivation of this work was to develop oxygenated g-C_3N_4 thin films without using any oxygen sources on purpose and utilize it for photocatalytic application. The magnetron sputtering has been considered so far as low cost, uniform deposition technique[13]. In this work, oxygen incorporation into g-C_3N_4 was attributed to the residual gas present in the sputtering chamber. This has been a new and cleaner way to make oxygenated g-C_3N_4.

The synthesis of oxygenated g-C_3N_4 thin films along with its characterization has been discussed briefly in the following section.

2 Materials and Methods

2.1 Experiment

Oxygenated g-C_3N_4 thin films were deposited on glass substrates at room temperature using an in-house fabricated DC magnetron sputtering system[14]. The setup was comprised of a non-magnetic stainless-steel chamber, an unbalanced magnetron sputter-head, target and substrate holders, and a vacuum system. A high-purity graphite target (99.99 %, 50 mm × 3 mm) was mounted beneath the magnetic assembly which was negatively biased, keeping the anode grounded. Approximately ~2 mm gap between the cathode and anode ensured a stable DC discharge for effective film deposition. The glass substrates were pre-cleaned with ethanol and then rinsed with Type-II deionized water to eliminate organic & inorganic residues. Then these were positioned approximately 20 mm below the target surface, secured on a substrate mounting table which was also maintained at ground potential. A Quadrupole Residual Gas Analyzer (PrismaPro,

*Corresponding author: E-mail: soumik.kundu@iem.edu.in

QMG 250 M2, 1–200 amu, Pfeiffer Vacuum, Germany) was connected with the system to study the experimental environment during synthesis. A Residual Gas Analyzer has a quadrupole-based mass spectrometer that was utilized to ionize gas molecules and identifies them by separating and measuring ions according to their mass-to-charge ratio. During synthesis, the chamber was evacuated and achieve a base vacuum pressure of 1.6×10^{-2} mbar using a two-stage anti-suck-back rotary vane vacuum pump. An operational pressure of 1.4×10^{-1} mbar was sustained within the system during the experiment by introducing a gas mixture of N_2 (Purity 99.999%) and H_2 (Purity 99.999 %) at a 10:1 ratio through the gas inlet. An operating power density of 0.97 W/cm^2 was achieved by maintaining a steady discharge current of about 40 mA at –480 Volt. The deposition was carried out for 30 minutes. During the sputtering process, both the gas atoms got energized in contact with the discharge plasma. The positive ions of hydrogen (H^+), generated through the ionization played an important role in sputtering the negatively biased graphite target[15]. The sputtered-out carbon atoms interacted with energized nitrogen atoms and residual gas components to create the thin films of oxygenated graphitic carbon nitride (O-g-C_3N_4). The mass spectrum during (1) stand-alone mode, (2) with a gas leak but no discharge and (3) with a gas leak during discharge was analysed across a scan range of 0–50 amu. During the stand-alone mode operation where QRGA was connected to the magnetron sputtering chamber without any external gas inject, the QRGA pressure was maintained at 4.0×10^{-7} mbar. Figure 1 (a) showed intensity peaks from the standalone QRGA system, indicating the presence of molecular hydrogen (H_2). Water vapour (H_2O) was also prominent and, upon ionization, dissociated into hydroxyl radicals ($O\dot{H}$) and atomic oxygen (O), as reflected in the spectrum. A peak at 28 amu likely corresponded to molecular nitrogen (N_2), while a smaller peak at 44 amu suggested trace of carbon dioxide (CO_2). Additionally, a distinct peak at 19 amu was attributed to hydronium ions (H_3O^+), likely formed through Electron Stimulated Desorption (ESD) caused by filament-emitted electrons interacting with nearby surfaces[16]. After the N_2+H_2 gas inlet inside the chamber, an operational pressure of 1.4×10^{-1} mbar was obtained. A controlled gas leak of 8.6×10^{-7} mbar was introduced from the magnetron sputtering system to facilitate mass spectrometry measurements using the QRGA setup. The mass spectrum before discharge and during discharge condition were observed and shown in Figs 1 (b) & (c). Significant change in mass peaks of molecular N_2 and H_2 gas were observed. A significant peak of atomic nitrogen was also observed at 14 amu. Prominent peaks of water vapour (H_2O), hydroxyl

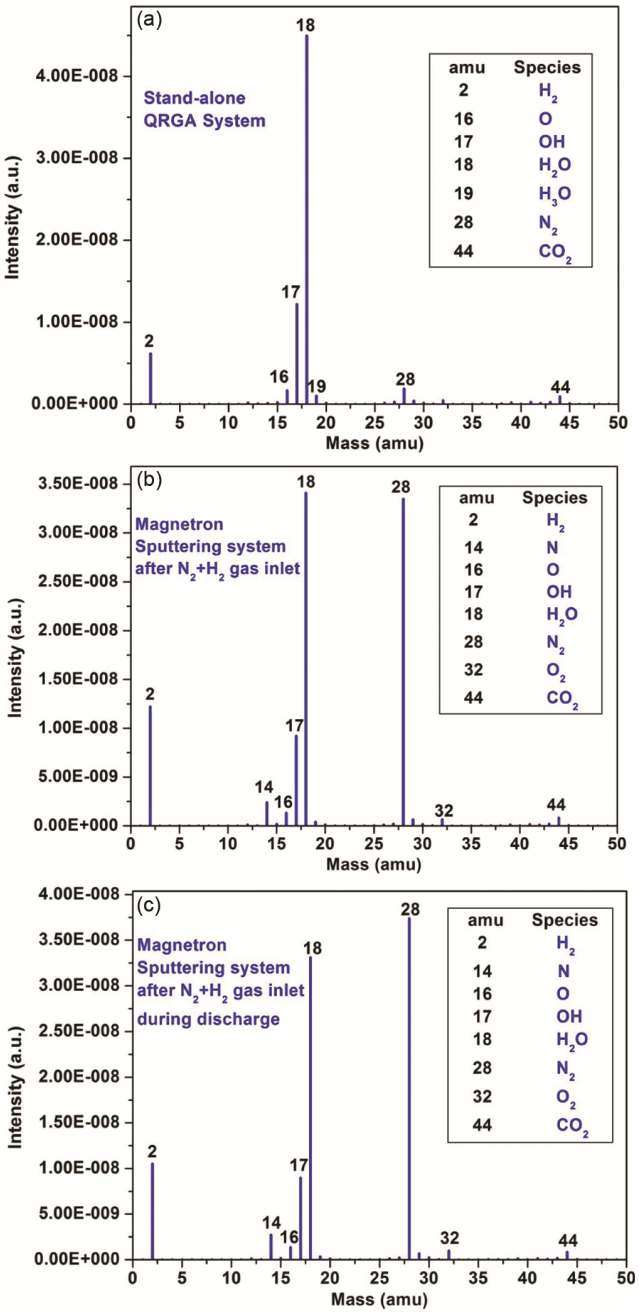

Fig. 1 — QRGA mass spectra (a) standalone system (b) Magnetron Sputtering System after N_2 + H_2 gas inlet during pre-discharge; and (c) Magnetron Sputtering System after N_2 + H_2 gas inlet during discharge

radicals (OḢ), atomic oxygen (O) and carbon di-oxide (CO_2) were also present during the synthesis. A small peak of molecular oxygen at 32 amu was also appeared. It was observed, the out gassing species e.g., OḢ, O, O_2 and CO_2 were only present inside the chamber which helped in oxygen incorporation and formation of oxygenated g-C_3N_4 thin films. There was no external oxygen supply into the reaction chamber occurred during this synthesis.

2.2 Characterization

The chemical composition of the samples was analyzed using XPS with Al Kα radiation (1486.7 eV), including a survey scan (0–1000 eV, 1 eV resolution) and high-resolution scans of C 1s, N 1s, and O 1s (0.2 eV resolution). Calibration of the XPS binding energy scale was performed using a gold sample. Raman spectroscopy was performed using a Lab RAM Horiba system with a 488 nm laser, covering 500–2500 cm^{-1}. Optical properties were examined using a Hitachi U-3900 UV-Vis spectrophotometer, recording absorption spectra from 350 to 800 nm. The most representative results were presented.

3 Results and Discussion

3.1 X-ray Photoelectron Spectroscopy Analysis

Figure 2 presented the XPS survey and high-resolution scans of C 1s, N 1s, and O 1s for the oxygenated g-C_3N_4 sample. The atomic percentage of 39 %, 33 % and 28 % was obtained for C, N, and O respectively. Core-level peaks were observed at 296.43 eV (C 1s), 409.29 eV (N 1s), and 541.77 eV (O 1s). The substrate work function (ϕ_{SA}) was estimated at 4.5 eV, consistent with g-C_3N_4[17]. Using the relation E_B=289.58−ϕ_{SA}[18], the corrected C 1s binding energy was calculated as 285.08 eV, indicating an 11.35 eV shift, which was applied to other core levels for accurate referencing. Deconvolution of the C 1s spectrum revealed four peaks at 284.4, 285.9, 287, and 287.8 eV, corresponding to sp^2 C=C, C–N/C–O, C=O, and N–C=N structures, respectively. N 1s peaks at 397.8, 399.1, and 401.02 eV indicated sp^2 aromatic nitrogen, C–N bonding, and N–H groups[19]. O 1s peaks at 530.7 and 532.6 eV suggest the presence of C=O and C–O bonds, likely induced by residual oxygen-containing species such as water vapour and CO_2 in the chamber, as shown in Fig. 1. These findings confirmed oxygen incorporation influenced by the synthesis environment.

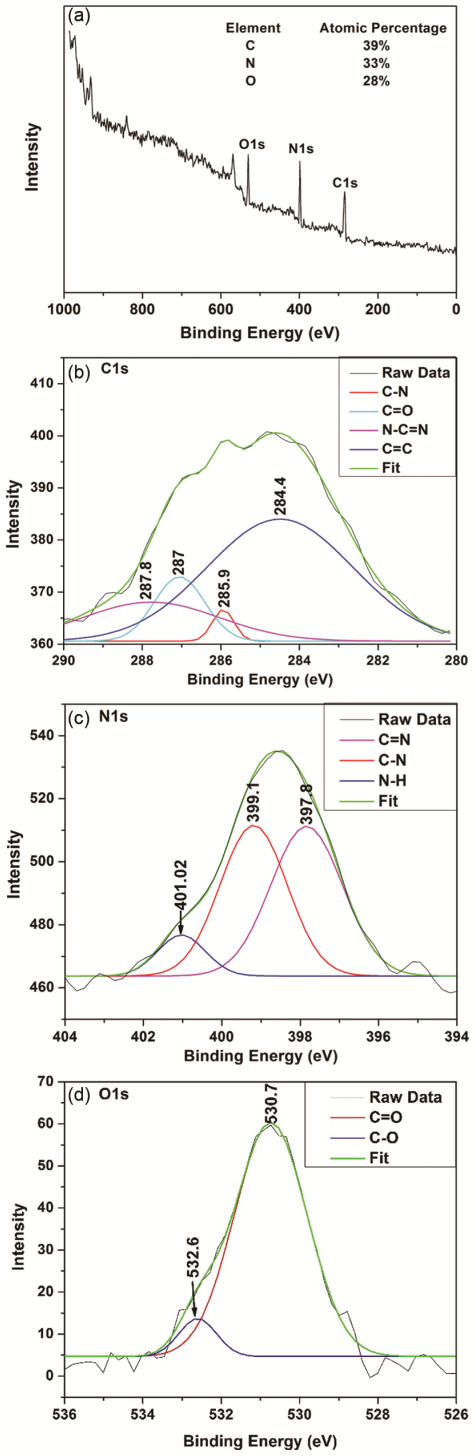

Fig. 2 — XPS analysis of g-C_3N_4 sample (a) survey scan (b) C 1s (c) N 1s; and (d) O 1s high-resolution spectra

3.2 Raman Spectroscopy Analysis

Raman spectroscopy was commonly employed to investigate the vibrational characteristics of carbon-based materials. The Fig. 3 has displayed the Raman spectra of a g-C_3N_4 film deposited on a glass substrate

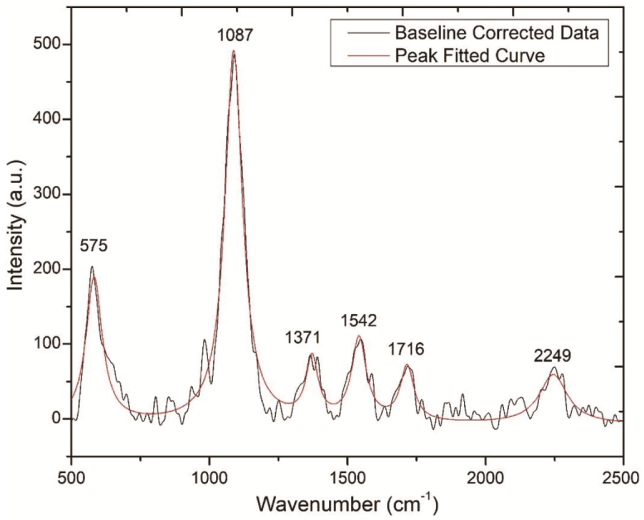

Fig. 3 — Raman spectra of the deposited g-C_3N_4 thin film

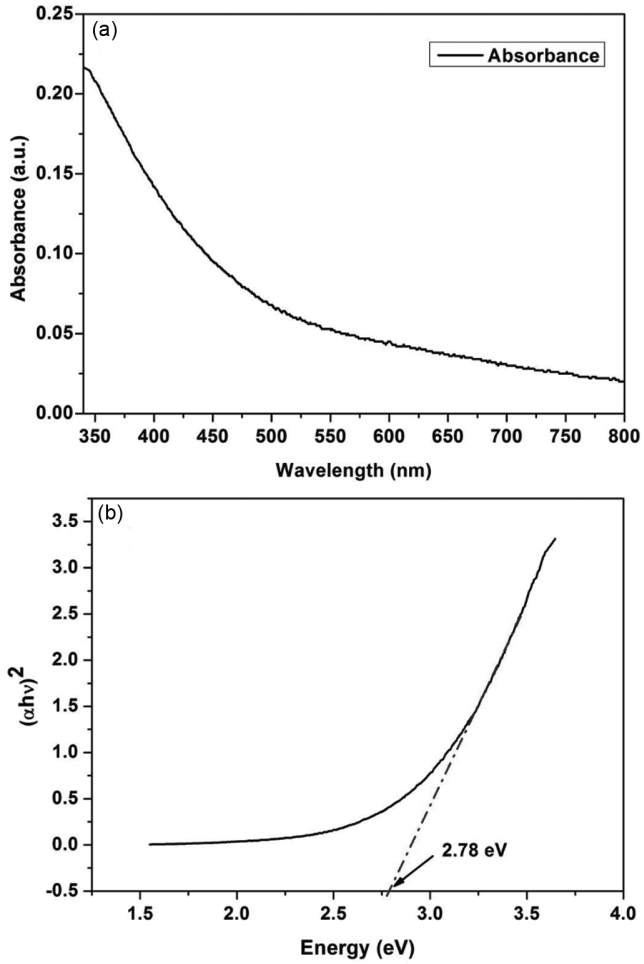

Fig. 4 — (a) UV-Vis absorption spectrum; and (b) optical band gap estimation using Tauc plot for g-C_3N_4 thin film

using a DC magnetron sputtering system. Several characteristic peaks of g-C_3N_4 were observed at 575, 1087, 1371, 1542 and 2249 cm^{-1}. The peak at 1542 cm^{-1} was attributed to its C=N stretching vibration, commonly referred to as the graphitic G band, signifying the development of a graphite-like structure. The 575 cm^{-1} peak were attributed to the in-plane symmetrical stretching vibration of heptazine heterocycles[20, 21]. The peaks at 1089 and 1371 cm^{-1} corresponded to the aromatic ring structure and D peak of the graphite structure respectively. The 2249 cm^{-1} peak, characteristic of carbon-nitrogen stretch, indicated that nitrogen was chemically bonded to carbon in the g-C_3N_4 film[22, 23]. The peak at 1716 cm^{-1} was attributed to the C=O bond formation due to presence of residual gas components during the synthesis at relatively high working pressure.

3.3 UV-Vis Spectroscopy Analysis

The investigation of photo absorption along with determination of optical bandgap was conducted by utilizing UV-Vis spectrophotometer and the results were illustrated in Fig. 4. The scan range was set between 350 and 800 nm. The photo absorption in visible range was observed from the spectrum as shown in Fig. 4 (a) which was very much required for better energy conversion and other photocatalytic applications. The bandgap was also calculated here using the Tauc plot method, which involved performing a linear regression on the graph of $(\alpha h\nu)^{1/n}$ versus hν, as per the Tauc Eq.[24]:

$$\alpha h\nu^{1/n} = A(h\nu - E_g) \quad \ldots (1)$$

In this context, α was the absorption coefficient, h represented the Planck constant, ν was the photon frequency, E_g signified the energy bandgap, n was the Tauc coefficient and A was the proportionality constant. The value of n was based on the type of electronic transition: for the direct transitions, n was ½, while for the indirect transition, n was 2. The g-C_3N_4 structure exhibits both direct and indirect bandgap property depending on its thickness. Here, a bandgap of 2.78 eV was obtained through direct transition method. In previous work, where pristine carbon nitride thin films have been developed on copper coated glass substrate using DC magnetron sputtering system at three different time spans under high vacuum condition. The bandgaps obtained from those samples were around 4 eV[25]. Here, the reduced direct bandgap of 2.78 eV was attributed to the induction of oxygen atoms in the structure[26]. The bandgap obtained from the graph displayed in Fig. 4 (b).

4 Conclusion

The characterization results indicated the formation of C–O and C=O, the basic bonding found in oxygenated g-C_3N_4 structure. The optical property also showed the effect of oxygen induction that helped in reducing bandgap and enhance the photocatalytic applications. But optimization in deposition parameter (i.e., deposition time, operating power and gas ratio) was planned to be carried out in future for developing highly efficient bulk sample. As the developed film has thin layer, the material content in the sample wasn't good enough for photocatalytic experiment such as dye degradation, the future scope of this work.

References

1 Balakrishnan A & Chinthala M, *Chemosphere*, 297 (2022) 134190.
2 Fernandes J, Kalluri S, Alsuwaidi M, Mayakrishnan V, Mohan C & Madhavan A A, *Chem Phys Imp*, 9 (2024) 100684.
3 Kolluru S, Prakash P V P R & Ramesh G V, *AIP Conf Proc*, 3361 (2025) 030027.
4 Wei F, *et al*., *Nanoscale*, 10 (2018) 4518.
5 Mishra S R, Gadore V & Ahmaruzzaman Md, *RSC Sustain*, 2 (2024) 91.
6 Chen W, Jiang D, Zhu M Y, Shi T Y, Li H N & Wang K, *J Alloy Compd*, 741 (2018) 1203.
7 Chen M, Bai R, Jin P, Li J, Yan Y, Peng A & He J, *J Alloys Compd*, 869 (2021) 159292.
8 Solgi S, Seyed Dorraji M S, Hosseini S F, Rasoulifard M H, Hajimiri I & Amani-Ghadim A, *Sci Rep*, 11 (2021) 19339.
9 Saka C, *Fuel*, 310 (2022) 122444.
10 Chubenko E B, Maximov S E, Bui C D, Pham V T & Borisenko V E, *Materialia*, 28 (2023) 101724.
11 Mishra S R, Gadore V & Ahmaruzzaman M, *Int J Environ Anal Chem*, 105 (2023) 315.
12 Li Y, Guo J, Han R & Wang Z, *Front Chem Sc Engg*, 18 (2024) 15.
13 Kelly P J & Arnell R D, *Vac*, 56 (2000) 159.
14 Taki G S, Kundu S K & Karmakar S, *IN Pat J*, 41 (2020) 52520.
15 Guan L, Xu N, Liu X, Zhao Y, Li H, Sun J, Wu J, & Ying Z, *Carbon*, 79 (2014) 578.
16 Cole C R, Outlaw R A, Champion R L, Holloway B C & Kelly M A, *Appl Surf Sc*, 253 (2007) 3789.
17 Zhu B, Cheng B, Zhang L & Yu J, *Carbon Energy*, 1 (2019) 32.
18 Greczynski G, *App Surf Sc*, 670 (2024) 160666.
19 Cao J, Qin C, Wang Y, Zhang H, Sun G & Zhang Z, *Mater*,10 (2017) 1.
20 Jiang J, Zhu L, Zou J, Ou-yang L, Zheng A & Tang H, *Carbon*, 87 (2015) 193.
21 Li H, Jing Y, Ma X, Liu T, Yang L, Liu B, Yin S, Wei Y & Wang Y, *RSC Adv*, 7 (2017) 8688.
22 Chen M Y, Li D, Lin X, Dravid V P, Chung Y W, Wong M S & Sproul W D, *J Vac Sc Tech*, *A* 11 (1993) 521.
23 Knight D S & White W B, *J Mater Res*, 4 (1989) 385.
24 Makuła P, Pacia M & Macyk W, *J Phys Chem Lett*, 9 (2018) 6814.
25 Kundu S K, Taki G S, 7th IEMENTech, 7 (2024) 581.
26 Tran D A, *et al*., *J Phys Chem Solids*, 151 (2021) 109900.